# Reaction enhancement of point sources due to vortex stirring

John P. Crimaldi,[1,*] Jillian R. Hartford,[1] and Jeffrey B. Weiss[2]

[1]*Civil and Environmental Engineering, University of Colorado, Boulder, Colorado 80309-0428, USA*
[2]*Department of Atmospheric and Oceanic Sciences, University of Colorado, Boulder, Colorado 80309-0311, USA*

We investigate a class of reactive advection-diffusion problems motivated by an ecological mixing process. We use analytical and numerical methods to determine reaction rates between two initially distinct scalar point masses that are separated from one another by a third (nonreactive) scalar. The scalars are stirred by a single two-dimensional vortex in a variety of geometrical configurations. We show that the aggregate second-order reaction rate in the low-concentration limit is enhanced by the instantaneous stirring processes, relative to the rate predicted by an equivalent eddy diffusivity. The peak reaction rate grows as $P^{1/3}$, and the time to reach the peak decreases as $P^{-2/3}$, where $P$ is the Péclet number. The results of this study have important implications not only for ecological modeling, but for the general understanding of turbulent reactive flows.

Chemical mixing and reaction rates in turbulent flows play a crucial role in many fields including ecology [1], atmospheric chemistry [2,3], combustion [4], and microfluidics [5]. The dual nonlinearities of fluid advection and chemical reaction rates combine to make this a particularly challenging problem. Most studies up to this point consider two scalars that are already in contact with one other in the initial condition. In one common scenario, the first scalar forms an island that is surrounded by the second scalar [3]; in another, each of the two scalars separately occupies one-half of the domain [6]. Results from this class of problems indicate that advective transport can enhance reaction rates between the two scalars, principally through filamentation that increases contact area between the neighboring scalars. In the present study, we investigate a different class of problems that has received little attention in the literature; namely, we consider two reactive scalars that are initially distinct, separated from one another by a third, nonreactive, scalar. This class of problems is inherently different because filamentation of the two reactive scalars by the advective field is not automatically accompanied by contact between those two species (since the third scalar can act as a spatial barrier). These different problems can have different scaling behavior: the separation between the two scalars introduces a length scale, while the case of scalars filling the two halves of the domain has no intrinsic length scale.

An ecological process called broadcast spawning motivated our study, and the process serves as an excellent example of this class of problems. Broadcast spawning is a fertilization strategy used by various benthic invertebrates (e.g., sea urchins, anemones, corals) whereby male and female adults release sperm and egg into the surrounding flow [7]. The sperm and egg (the two reactive scalars) are initially separated by ambient water (the third, nonreactive, scalar). For effective fertilization, the turbulent stirring must not just produce filaments of the reactive scalars, it must also bring these filaments (from the initially distinct scalars) into close contact.

The aggregate effect of instantaneous turbulent stirring and mixing is often modeled using an eddy viscosity (for momentum) or an eddy diffusivity (for scalars). While this method is sometimes satisfactory, it is intrinsically a time-averaged approach that can fail spectacularly. For example, in the broadcast spawning problem, field measurements of fertilization rates are rarely less than 5%, and are often as high as 90% [8–10]. However, numerical modeling based on a turbulent eddy diffusivity predicts fertilization rates of only 0.01–1 %, due to the strong time-average turbulent dilution of the gametes [11]. Many studies [3,12] have shown that the instantaneous details of advective transport (not captured by the eddy diffusivity approach) can enhance reactions rates for scalars that are initially in contact. We hypothesize that similar reaction enhancements are produced in problems like broadcast spawning, even though the reactive scalars are initially distinct. The results of this study have important implications not just for ecological modeling, but for the general understanding of turbulent reactive flows.

By way of introduction, consider the turbulent transport of two scalars $A$ and $B$. Each local scalar concentration $C_A$ and $C_B$ can be decomposed into mean and fluctuating components $C(t) = \bar{C} + c'(t)$. For simplicity, we assume that $C_A$ and $C_B$ react at the second-order rate $kC_AC_B$, where $k$ is the dimensional reaction rate constant. At any location, the time-averaged value of the reaction rate is then

$$\overline{kC_A(t)C_B(t)} = k\overline{C_A C_B} + k\overline{c'_A(t)c'_B(t)}, \qquad (1)$$

where the first term on the right-hand side is simply the product of the time-averaged concentrations, and the second term is the correlation between the fluctuating concentrations. By definition, models based on an effective turbulent diffusivity incorporate only the first term. The question then becomes, is the second term nonzero, and why? In this paper we examine the ability of structured stirring processes to impose scalar correlations on initially distinct point scalar masses.

The basic mechanism by which advection can increase the reaction rate is simple, in principle. For incompressible flows, turbulent stirring can only stretch and fold scalar filaments, with no direct mechanism for decreasing the filament

_____

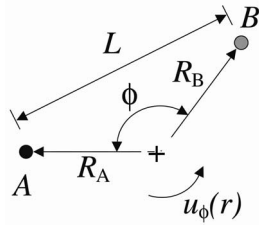*Author to whom correspondence should be addressed. Electronic address: crimaldi@colorado.edu

FIG. 1. Geometry for two-scalar vortex stirring problem.



FIG. 2. Numerical simulations of $\Theta$ vs $t$ for $P=0,10,100$. The $P=0$ results match Eq. (3), which is shown with a dashed line.

concentration. Only molecular diffusion intersperses fluid between adjacent filaments to produce scalar dilution. Thus, the parametrization of advective stirring by an eddy diffusion is intrinsically flawed since it incorrectly produces a systematic decrease in concentrations and thus a decrease in reaction rates. If, on the other hand, advection brings two scalar filaments together before molecular diffusion decreases their concentration, then the reaction rate will be enhanced.

Oceanic flows tend to be populated by coherent vortices with long lifetimes. We thus consider the problem of two reactive point-source scalars stirred by a vortical flow $u_\phi(r)$ (see Fig. 1). The point masses are placed at distances $R_A$ and $R_B$ from the vortex center, with initial angular and linear separations $\phi$ and $L$. Both scalars have mass $M$ and molecular diffusivity $D$.

We consider only the low-concentration limit where the scalar concentrations are small and the second-order reactive removal of scalar mass is negligible. The total dimensional reaction rate $\hat{\Theta}(t)$ corresponds simply to the scalar overlap integrated over the domain:

$$\hat{\Theta}(t) = \iint k C_A C_B dA. \qquad (2)$$

To establish a baseline case that excludes instantaneous stirring processes, we first consider the case of pure diffusional spreading ($u_\phi=0$) due to molecular diffusion. We work in nondimensional variables where we scale time by a diffusive time $t_d=L^2/8D$, distances by $L$, and the total reaction rate by $kM^2/\pi e L^2$. The resulting expression for $\Theta$ in the low-concentration limit is [13]

$$\Theta = \frac{e}{t} \exp\left(-\frac{1}{t}\right). \qquad (3)$$

With this scaling, $\Theta$ reaches its peak value of unity at $t=1$. Equation (3) is shown as the dashed line in Fig. 2. For small times, $\Theta$ is effectively zero due to the initially distinct scalars, and, at large times, $\Theta$ asymptotes to zero due to diffusional dilution of $C_A$ and $C_B$. It is only at intermediate time scales that diffusion has produced enough spreading for interactions between the scalars, but not so much spreading that they become overly dilute.

To consider the effect of structured stirring processes, we now add an ideal point-vortex velocity field $u_\phi(r)$ $=\Gamma/(2\pi r)$, where $\Gamma$ is the vortex circulation. The advective time scale based on one revolution at $r=R\equiv(R_A+R_B)/2$ is $t_a=2\pi R^2/\Gamma$. This leads to a Péclet number
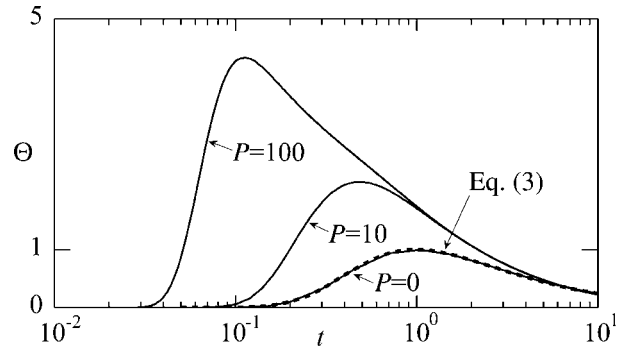
$$P = \frac{t_d}{t_a} = \frac{\Gamma}{4\pi D}\left(\frac{L}{2R}\right)^2, \qquad (4)$$

where $P=0$ corresponds to the pure diffusion case and $P$ becomes large as advection dominates.

We first determine $\Theta$ for the simplest case $R_A=R_B=L/2$ and $\phi=\pi$, such that $P=\Gamma/4\pi D$. In the limit of large $P$, $\Theta$ can be calculated analytically. Due to the radial shear of the vortex, particles are rapidly dispersed in the circumferential direction by shear dispersion [14]. For large $P$, the radial diffusion is small, the nonlinear dependence of the velocity on radius is well approximated by its linear shear, and the polar geometry $(r,\phi)$ can be approximated by a periodic Cartesian geometry $\mathbf{x}=(x,y)$. The velocity is then $\mathbf{u}=(-\sigma y,0)$, and the shear is $\sigma=\Gamma/\pi R^2=16PD/L^2$. Thus, in the large-$P$ limit, the problem depends only on the local shear, independent of other aspects of the vortex profile.

In a nonperiodic Cartesian geometry an initial $\delta$-function point source at the origin evolves under a linear shear into a Gaussian concentration $C(\mathbf{x},t)=N\exp(\mathbf{x}\mathbf{A}^{-1}\mathbf{x}/2)$, where $\mathbf{A}$ is the covariance matrix,

$$\mathbf{A} = \begin{pmatrix} P^2t^3/3 & -Pt^2/4 \\ -Pt^2/4 & t/4 \end{pmatrix}, \qquad (5)$$

and $N$ is a normalization factor. Note that the $P^2t^3$ shear dispersion in the $x$ direction dominates over the linear-in-time dispersion in the $y$ direction.

For the periodic Cartesian geometry intrinsic to vortex stirring, the periodic images of $C$ must be summed. The sum in the resulting integral, Eq. (2), gives the Jacobi elliptic theta function $\vartheta_2(z,q)$ [15]. The reaction rate for different Péclet numbers is self-similar for large $P$, and the explicit dependence on $P$ can be eliminated by using the similarity variables $\Theta_s=\Theta P^{-1/3}$, and $t_s=tP^{2/3}$, giving

$$\Theta_s(t_s) = \frac{\sqrt{3}e}{t_s^2} \vartheta_2\left(0,\exp\left[\frac{-3\pi^2}{t_s^3}\right]\right). \qquad (6)$$

Equation (6) is shown as the dashed line in Fig. 3. The peak reaction rate grows as $P^{1/3}$, while the time to reach the peak shrinks as $P^{-2/3}$, indicating that vortex stirring can produce significant amplification and acceleration of the reaction over pure diffusion. A similar analysis for two scalars filling two halves of an infinite domain gives, due to the lack of a length
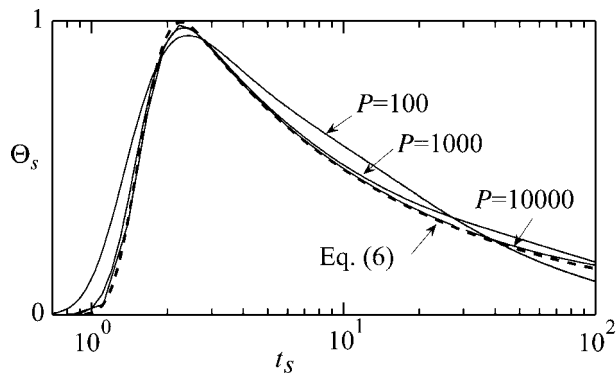
FIG. 3. Simulation results for large Péclet numbers, plotted in self-similar variables. As $P$ increases, the simulation results approach Eq. (6), shown with the dashed line.

scale, a similarity solution where different values of shear and diffusion give the same solution but at a different time, which is qualitatively different from the scaling with $P$ seen here for two point sources.

Turbulent stirring is often parametrized by eddy diffusion. If stirring does act diffusively, then one can choose an eddy diffusivity $D_e$ so the diffusive time scale for the eddy diffusivity matches the advective time scale, $D_e = PD$. The reaction rate for a process governed by such an eddy diffusion is the diffusive reaction rate Eq. (3), with time scaled by $P$:

$$\Theta(t) = \frac{e}{Pt} \exp\left(-\frac{1}{Pt}\right). \tag{7}$$

The peak reaction rate is still unity, but occurs at an accelerated time which scales as $P^{-1}$. Eddy diffusion can thus speed up reactions, but since it necessarily spreads scalars as they diffuse, it cannot enhance the reaction rate over the values attained under molecular diffusion. This illustrates the fundamental failure of eddy diffusion models of turbulent stirring of reactive scalars.

With analytical $\Theta$ expressions now defined for $P=0$ [Eq. (3)], and for large $P$ [Eq. (6)], we now turn to a numerical modeling approach to calculate $\Theta$ for a range of intermediate $P$ values. The model uses a Lagrangian particle-tracking approach, with a random-walk model for molecular diffusion. The two-dimensional position of a particle $\mathbf{x}_n$ is determined from its previous position $\mathbf{x}_{n-1}$ using the updating relationship [16]

$$\mathbf{x}_n = \mathbf{x}_{n-1} + \mathbf{u}(\mathbf{x}_{n-1})\Delta t + \mathbf{Z}\sqrt{2D\Delta t}, \tag{8}$$

where $\mathbf{u}$ is the local velocity vector, and $\mathbf{Z}$ is a two-dimensional random vector with mean magnitude zero and variance one. The particle-tracking method does not exhibit any numerical dispersion in the classical sense [16], and the computational effort is proportional to the number of particles and is therefore concentrated into areas with the highest concentrations [17]. In the simulation, we vary $P$, but hold $kM/D$ (a Damkoler number) constant at unity.

Simulation results for $\Theta$ vs $t$ for $P=0$, 10, and 100 are shown in Fig. 2, again for the simplest case $R_A = R_B = L/2$ and $\phi = \pi$. The enhancement and acceleration of the reaction rate
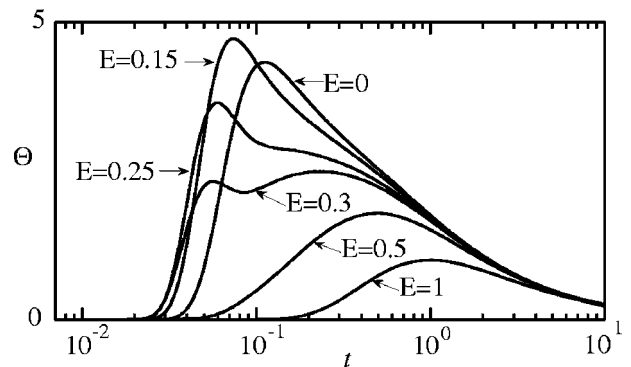


FIG. 4. Simulations of $\Theta$ for eccentric ($E \neq 0$) initial conditions at $P=100$ and $\phi = \pi$.

as $P$ increases are evident. The $P=0$ simulation matches the pure-diffusion analytical solution [Eq. (3)], shown by the dashed line. Simulation results for higher Péclet numbers are shown in Fig. 3, this time plotted in self-similar coordinates. As $P$ increases, the simulation results approach the high-Péclet analytical solution [Eq. (6)], shown with the dashed line.

In order to test the effects of the initial geometric placement of scalars $A$ and $B$ on the reaction rate, we now vary the initial geometry of the scalars relative to the vortex. The relative radii of the initial scalar positions is described by an eccentricity

$$E = \frac{R_A - R_B}{R_A + R_B}, \tag{9}$$

where $E=0$ is a symmetric initial condition, and $E=1$ is the limiting case where one scalar mass coincides with the vortex center. Simulation results for $\Theta$ for six values of $E$ at $P=100$ and $\phi = \pi$ are shown in Fig. 4.

As $E$ increases from zero, the peak value of $\Theta$ first increases (as seen in the $E=0.15$ curve) and then decreases. As $E$ approaches unity, the $\Theta$ curve reverts to the pure diffusion solution. For intermediate values of $E$, two local $\Theta$ maxima occur. The first maximum corresponds to an asymmetric distribution of scalar overlap [the integrand of Eq. (2)] as the leading edge of one of the scalar filaments overtakes the trailing edge of the second (see Fig. 5).

The second maximum corresponds to a largely symmetric overlap distribution as radial diffusion dominates the scalar dispersion. The nondimensional reaction rate $\Theta$ is insensitive to changes in the initial angle $\phi$ for the pure diffusion case, but it becomes increasingly sensitive as $P$ increases. The variation of the peak value of $\Theta$ as a function of $\phi$ is shown for three values of $P$ in Fig. 6(a).

Finally, we consider the significance of the chosen vortex velocity distribution $u_\phi(r)$ on $\Theta$. An interesting comparison case is the distribution given by $u_\phi(r) = (\Gamma/2\pi r)\{1 - \exp[-(2r/B)^2]\}$. Often called an Oseen vortex, this distribution behaves like the ideal point vortex when $2r/B \gg 1$, and like solid-body rotation when $2r/B \ll 1$. Figure 6(b) is a plot of the peak value of $\Theta$ in an Oseen vortex for $P=1000$ and $\phi = \pi$ as a function of initial scalar separation $L/B$. When the scalars are placed outside the rotational core of the vortex
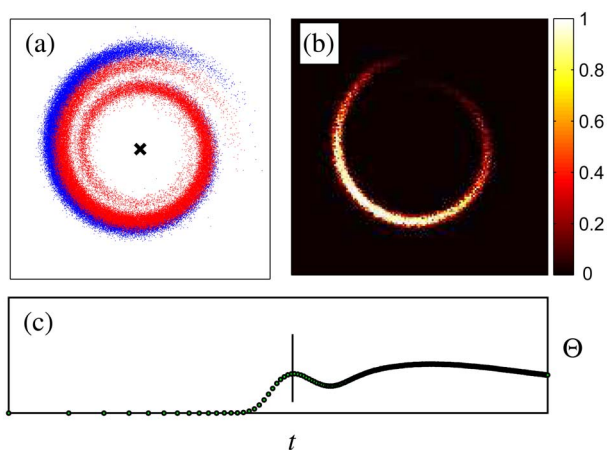
FIG. 5. (Color online) Snapshots of a simulation for $P=1000$, $E=0.16$, and $\phi=\pi$ showing (a) scalar $A$ [red (light gray)] and $B$ [blue (dark gray)] particle locations, (b) distribution of the scalar overlap [the integrand of Eq. (2)], and (c) the time (shown by the vertical line) of the snapshots.

$(L/B \gg 1)$, $\Theta$ has the same enhancement and acceleration as the ideal vortex result. However, when the scalars are placed inside the core, where there is no straining (and hence no shear dispersion), $\Theta$ reverts to the unenhanced pure diffusion result.

The results presented in this paper demonstrate that instantaneous stirring processes have a profound impact on reaction rates between two initially distinct point scalars. Stirring imparts spatial correlations from the velocity field onto the initially uncorrelated scalar field. This structured stirring results in enhanced reaction rates that are not predicted by eddy diffusivity models, even when the average scalar variance growth is modeled correctly. The reaction enhancement is highest at intermediate time scales, when scalar filaments are stirred into close proximity but are not yet strongly diffused. Any eddy diffusivity approach (regardless of the diffusivity magnitude) will produce the same reaction rates as the $P=0$ pure diffusion case shown in Fig. 2, with no reaction enhancement. Thus, the results indicate a fundamental
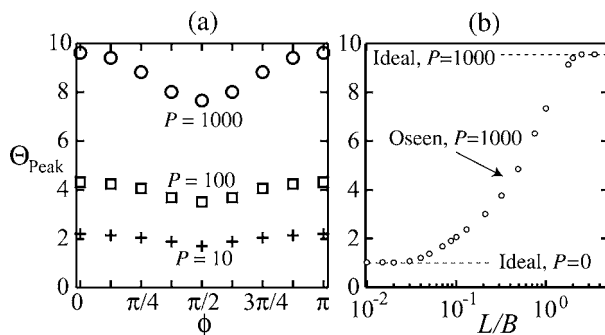


FIG. 6. Sensitivity of the peak value of $\Theta$ to (a) variations in the initial angle $\phi$ for the ideal vortex for $P=10$, 100, and 1000, and (b) variations of the initial scalar separation $L/B$ in an Oseen vortex for $\phi=\pi$ and $P=1000$. The dashed lines indicated the peak $\Theta$ values for an ideal point vortex at $P=0$ and 1000.

flaw in relying on time-averaged techniques such as eddy diffusion when modeling these types of reactions.

Although we chose an extremely simplistic velocity field (to facilitate both analytical and numerical approaches), the results suggest similar implications for more generalized flowfields. If turbulence is conceptualized as a collection of interactive vortices, then, at local scales, the instantaneous flow fields resemble those used in this study. In this case, two reactive scalars in the vicinity of a vortex are likely to experience reaction enhancement and acceleration analogous to that presented in the study. The relative insensitivity of the results to the initial geometry of the scalars facilitates this extension. Indeed, preliminary simulations of two-dimensional flows with multiple, interactive vortices exhibit enhanced reaction rates relative to that predicted by an eddy diffusivity approach. Detailed studies are needed to assess possible extensions of these results in two- and three-dimensional flows.

[1] A. Okubo and S. A. Levin, *Diffusion and Ecological Problems: Modern Perspectives*, 2nd ed. (Springer-Verlag, New York, 2001).

[2] S. F. Maria, L. M. Russell, M. K. Gilles, and S. C. B. Myneni, Science **306**, 1921 (2004).

[3] S. Edouard, B. Legras, and V. Zeitlin, J. Geophys. Res., [Atmos.] **101**, 16771 (1996).

[4] N. Peters, *Turbulent Combustion* (Cambridge University Press, Cambridge, U.K., 2000).

[5] V. Hessel, H. Lowe, and F. Schonfeld, Chem. Eng. Sci. **60**, 2479 (2005).

[6] F. J. Muzzio and M. Liu, Chem. Eng. J. **64**, 117 (1996).

[7] D. Levitan, in *Ecology of Marine Invertebrate Larvae*, edited by L. McEdward (CRC Press, Boca Raton, FL, 1995), pp. 123–156.

[8] J. E. Eckman, J. Exp. Mar. Biol. Ecol. **200**, 207 (1996).

[9] J. Pennington, Biol. Bull. **169**, 417 (1985).

[10] P. Yund, Trends Ecol. Evol. **15**, 10 (2000).

[11] M. W. Denny and M. F. Shibata, Am. Nat. **134**, 859 (1989).

[12] J. M. Ottino, Chem. Eng. Sci. **49**, 4005 (1994).

[13] J. P. Crimaldi and H. S. Browning, J. Mar. Syst. **49**, 3 (2004).

[14] G. Taylor, Proc. R. Soc. London, Ser. A **219**, 186 (1953).

[15] *Handbook of Mathematical Functions: With Formulas, Graphs, and Mathematical Tables*, edited by M. Abramowitz and I. A. Stegun (Dover Publications, New York, 1974).

[16] W. Kinzelbach, in *Groundwater Flow and Quality Modeling*, edited by E. Custodio (Reidel, Rotterdam, 1988), pp. 227-245.

[17] K. Dimou and E. Adams, Estuarine Coastal Shelf Sci. **37**, 99 (1993).